

AD-787 875

LAMELLAR COMPOSITES FORMED BY
SPUTTER DEPOSITION

R. A. Busch, et al

Battelle-Pacific Northwest Laboratories

Prepared for:

Air Force Office of Scientific Research

July 1974

DISTRIBUTED BY:

NTIS

National Technical Information Service
U. S. DEPARTMENT OF COMMERCE

UNCLASSIFIED

SECURITY CLASSIFICATION OF THIS PAGE (When Data Entered)

REPORT DOCUMENTATION PAGE		READ INSTRUCTIONS BEFORE COMPLETING FORM
1. REPORT NUMBER AFOSR - TR - 74 - 1595	2. GOVT ACCESSION NO.	3. RECIPIENT'S CATALOG NUMBER AD-787 875
4. TITLE (and Subtitle) LAMELLAR COMPOSITES FORMED BY SPUTTER DEPOSITION		5. TYPE OF REPORT & PERIOD COVERED INTERIM 1 May 1973-30 April 1974
		6. PERFORMING ORG. REPORT NUMBER ARPA Order No 2482
7. AUTHOR(s) R A BUSCH J W PATTEN		8. CONTRACT OR GRANT NUMBER(s) F44620-73-C-0071
9. PERFORMING ORGANIZATION NAME AND ADDRESS BATTELLE, PACIFIC NORTHWEST LABORATORIES BATTELLE BOULEVARD, PO BOX 999 RICHLAND, WASHINGTON 99352		10. PROGRAM ELEMENT, PROJECT, TASK AREA & WORK UNIT NUMBERS 681307 9782-05 61102F
11. CONTROLLING OFFICE NAME AND ADDRESS AIR FORCE OFFICE OF SCIENTIFIC RESEARCH/NA 1400 WILSON BOULEVARD ARLINGTON, VIRGINIA 22209		12. REPORT DATE July 1974
		13. NUMBER OF PAGES 57
14. MONITORING AGENCY NAME & ADDRESS (If different from Controlling Office)		15. SECURITY CLASS. (of this report) UNCLASSIFIED
		15a. DECLASSIFICATION/DOWNGRADING SCHEDULE
16. DISTRIBUTION STATEMENT (of this Report) Approved for public release; distribution unlimited.		
17. DISTRIBUTION STATEMENT (of the abstract entered in Block 20, if different from Report)		
18. SUPPLEMENTARY NOTES Reproduced by NATIONAL TECHNICAL INFORMATION SERVICE U S Department of Commerce Springfield VA 22151		
19. KEY WORDS (Continue on reverse side if necessary and identify by block number) LAMELLAR COMPOSITES SPUTTER DEPOSITION COPPER-MOLYBDENUM BERYLLIUM-TITANIUM		
20. ABSTRACT (Continue on reverse side if necessary and identify by block number) Data and results from the first year's evaluation of two types of lamellar composites is presented and discussed.		

DD FORM 1473

JAN 73

EDITION OF 1 NOV 65 IS OBSOLETE

UNCLASSIFIED

SECURITY CLASSIFICATION OF THIS PAGE (When Data Entered)

LAMELLAR COMPOSITES FORMED BY SPUTTER DEPOSITION

Annual Technical Report

June 1974

Sponsored by Advanced Research Projects Agency

Contract No. F44620-73-C-0071
Modification P00003, July 8, 1974
ARPA Order No. 2482
Program Code No. 3D10

Principal Investigator
H. R. Gardner
509-942-2305

Program Managers
R. A. Busch
509-942-2685

J. W. Patten
509-942-2603

Contract Technical Monitor
Wm. Walker

Effective Date
May 1, 1973

Contract Expiration Date
April 30, 1975

Amount of Contract
\$245,000

BATTELLE
PACIFIC NORTHWEST LABORATORIES
RICHLAND, WASHINGTON 99352

CONTENTS

LIST OF FIGURES	iv
LIST OF TABLES	v
INTRODUCTION	1
SUMMARY	2
TECHNICAL PROBLEM	2
Thin-Layered Systems	2
Compound Forming Systems	3
GENERAL METHODOLOGY	4
TECHNICAL RESULTS	4
Thin-Layered Systems	4
Compound Forming Systems	6
THIN-LAYERED SYSTEMS	8
MATERIALS AND PROCEDURES	8
Deposition	8
Heat Treatment	9
Evaluation	12
X-Ray Diffraction	12
Transmission Electron Microscopy	13
Hardness Testing	13
Tensile Testing	13
Other Techniques	14
RESULTS AND DISCUSSION	14
Deposition	14

Evaluation	15
X-Ray Diffraction	15
Transmission Electron Microscopy	20
Hardness Testing	23
Room Temperature Hardness	23
Hot Hardness	28
Calculation of Ultimate Tensile Strength From Hot Hardness	30
Tensile Properties	32
Scanning Electron Microscopy	33
COMPOUND FORMING SYSTEMS	33
MATERIALS AND PROCEDURES	33
RESULTS AND DISCUSSION	37
Deposit Quality	37
Mechanical Properties	37
Tensile	37
Three Point Bending	42
General Evaluation	45
REFERENCES	50

LIST OF FIGURES

1	Sputtering Hardware for Deposition of Lamellar Composites.	10
2	Approximate Configuration of 65 and 95°C Deposits After Removal from the Substrate Holder	16
3	Diffraction Patterns of OTLC-2, As Sputtered	17
4	Unicam X-Ray Diffraction Pattern of OTLC-2, As-Sputtered. Note (111) Cu (left arrow) and (110) Mo (right arrow) Peak Splitting	19
5	TEM Micrographs of OTLC-2, Heat Treated at 500°C for 3 Hours. Viewed Parallel to Layer Planes.	21
6	TEM Micrographs of OTLC-2, Heat Treated at 1000°C for 4 Hours. Viewed Parallel to Prior Layer Planes	22
7	TEM Micrographs of OTLC-2, Heat Treated at 750°C for 2 Hours. Viewed Parallel to Prior Layer Planes	24
8	TEM Micrograph of OTLC-2 Heat Treated at 1000°C for 2 Hours. Viewed Parallel to Prior Layer Planes. Mo Spheres are Approximately 2130 Å in Diameter	24
9	Room Temperature DPH Versus Time at Heat Treating Temperature	25
10	Room Temperature DPH Versus Heat Treating Temperature for Several Heat Treating Times	26
11	Arrangement of Sputtering Targets for the Deposition of Ti + BeTi Lamellar Composites. The Titanium and Beryllium Targets are Electrically Independent; the Substrate is Concentric with the Targets and Rotates	35
12	Cross Section of Typical Lamellar Composite	38
13	Fracture Surface of Tensile Specimen from Deposit 24/0.2. Scanning Electron Micrographs. Note Absence of Delamination in D	41
14	Fracture Surfaces of Bend Specimens from Deposits: a) 14/0.1, b) 24/0.1. Scanning Electron Micrographs	44

15	Cross Section of Deposit after Heat Treatment at 950°C for One Hour. The Lamellar Structure has Broken Up by Diffusional Processes. Optical Micrograph 100X	46
16	Microhardness of Lamellar Composites as a Function of Heat Treatment	47

LIST OF TABLES

I	Properties of the Components of the Lamellar Composite	8
II	Deposition History and Comment	11
III	Heat-Treatment Parameters for Deposits TLC-4, TLC-2, and OTLC-2 . .	12
IV	Influence of Heat Treatment on Microstructure of Deposit OTLC-2 . .	23
V	Room Temperature DPH Hardness Measurements	27
VI	Influence of Temperature on Hot Hardness of TLC-2	29
VII	Elevated Temperature Ultimate Tensile Strengths (σ_u) of Cu-Mo Laminate, Cu, Mo, and Cu-2%ThO ₂	31
VIII	Calculated Characteristics of Ti-BeTi Lamellar Composites	36
IX	Tensile Properties of Lamellar Composites	39
X	Bend Test Results	42
XI	Electrical Resistivity of Deposit 14/0.1 as a Function of Heat Treatment	48

INTRODUCTION

This report describes the progress made during the second half of Phase I of the investigation of lamellar composites formed by sputter deposition of alternate layers of selected two component systems. Some of the data reported in the first Semiannual Technical Report, covering the progress made during the first half of Phase I, is also included in the interest of clarity. Phase I is the first of a proposed three-year, three-phase program being conducted by Battelle Northwest Laboratories.

The purpose of this investigation is to evaluate the potential of two approaches to produce the lamellar composites. In each approach the favorable properties of both components will be used to obtain properties which neither component has initially. In one approach a thin-layered system is being explored in which strengthening is derived from the interface effects and small thickness of individual layers. In the other approach a thicker layered compound-forming system is being explored. This system is strengthened by the bulk properties of the component materials and their reaction products as modified by the constraints of bonding to each other. The dividing line in layer thickness between the two systems is felt to be about 1000 Å.

Both types of composites are expected to exhibit yield strengths on the order of one percent or more of the elastic modulus of the composite material. The range of mechanical properties obtainable is expected to depend on the difference in elastic modulus between the component materials, the relative and absolute thickness of the layers, and the deposition conditions employed.

Sputter deposition offers a unique process for producing lamellar composites. It can precisely and reproducibly control individual component layer thicknesses down to tens of atom layers. This can provide control over macroscopic properties through layer thickness effects. A second feature of sputtering is its ability to achieve interlayer bond strengths of the order of the material strength and thereby attain good load transfer across the matrix interface. With respect to production, a single sputter-deposition apparatus can form a deposit of one millimeter thickness over an area of approximately 500 cm² in a 24-hour day.

SUMMARY

TECHNICAL PROBLEM

The objective of the program is to develop new composites which utilize the favorable properties of the materials they combine to produce properties which neither component originally has. Mechanical properties and their thermal stability are of primary interest for assessment of usefulness in engineering applications.

Thin-Layered Systems

Koehler⁽¹⁾ has proposed the design of a strong solid composed of alternate layers of materials with high and low elastic constants. He expects yield strengths on the order of one percent of the elastic modulus if layers are thin enough ($\sim 200 \text{ \AA}$) to prevent the operation of Frank-Reed sources. It also has been shown⁽²⁻⁴⁾ that up to 20 \AA of a pure metal may assume the crystal structure of another metal upon which it has been deposited. This is referred to as pseudomorphic or epitaxial growth. The boundary region of such a film would be very highly

stressed in the same manner as are Guinier-Preston zones or boundaries of other coherent precipitates.

The object of the thin-layered system program is to fabricate lamellar composites with layers less than 200 Å thick. These layers would consist of two metals mutually insoluble in the solid state, with different crystal structures and with widely different elastic moduli and coefficients of thermal expansion. Contributions to a high level of internal stress should be realized from lattice distortion produced by pseudomorphic layers, fine grain size and high internal stress levels achievable in pure sputtered materials, and property mismatch. It is not expected that Frank-Reed sources will operate within a given layer; therefore, dislocations should be very difficult to generate. The long-range nature of the dislocation barriers (layer interfaces) together with the need to preserve Burgers vector in moving across an interface should also make dislocation movement very difficult. Vacancy diffusion to the interfaces and subsequent defect movement should provide the only deformation mechanism.

Compound-Forming Systems

Compound-forming systems do not depend on the small dimensions of the layers for their properties. The elements or compounds forming the layers are selected for their individual properties and their compatibility with each other. The reinforcing layer consists of a high elastic modulus material such as an oxide, carbide or intermetallic compound; the other layer is a metal with a reasonable degree of plasticity. These composites could function similarly to existing composite materials in that the metal would protect, orient, and transfer load to

the reinforcing layer. They would be expected to achieve higher strengths than existing composites due to the strong bonding between layers. They may, however, suffer the drawback of a potential continuous crack path in the brittle reinforcing layer.

GENERAL METHODOLOGY

The general approach is experimental. Tensile testing and microhardness techniques are being used to study mechanical properties as a function of relative and absolute laminate layer thickness, substrate temperature during deposition, and heat treatment temperature after deposition. In addition such techniques as x-ray diffraction, scanning electron microscopy, calorimetry, and resistivity measurements are being used to gain insight into structure, fracture behavior, and other composite characteristics as a function of time and temperature.

Depositions on large cylindrical substrates will be performed to provide tensile samples and additional material for metallurgical characterization.

TECHNICAL RESULTS

Thin-Layered Systems

Data obtained to date indicate that the thin laminate structure provides a very effective new strengthening mechanism. X-ray diffraction results for depositions made at less than 100°C indicate that the structure, particularly in the interface region, is highly strained. No phases other than bcc Cu and fcc Mo were observed. Very strong Cu (111) and Mo (110) textures were observed perpendicular to the plane of the layers. Transmission electron microscopy (TEM) and electron

diffraction data indicate that a very high integrity layered structure with distinct and continuous alternating layers of Cu and Mo was obtained on sputter deposition. Each of these layers was 50-100 Å thick and was composed of equiaxed grains 50-100 Å in diameter. The layered structure withstood a heat treatment of 4 hours at 500°C but broke down by spheroidization of the Mo after 2 hours at 750°C. The spheroidized structure after this heat treatment consisted of 860 Å diameter Mo spheres in a twinned Cu matrix. The Mo spheres grew in diameter with increasing time at temperature with 3000 Å diameter Mo spheres being observed after 4 hours at 1000°C. Room temperature hardness of as-deposited samples was in excess of 625 DPH, which is much higher than that observed in either pure Cu or pure Mo. Hardness decreased with heat treatment above 650°C, which may indicate the onset of Mo spheroidization, but room temperature hardness of a sample spheroidized by heat treatment at 1000°C for 4 hours was still greater than the values observed for as-rolled Mo bar stock. Calculations based on hardness measurements indicate that, at room temperature, the Cu-Mo laminate structure is much stronger than either pure Cu or pure Mo and is roughly 3 times stronger than expected by the rule of mixtures. Further the calculated as-deposited composite σ_u of 16,918 kg/cm² (240,625 lbs/in²) based on 625 DPH hardness, is approximately 0.48% of the modulus of Mo, 0.72% of the modulus expected by the rule of mixtures and 1.1% of the observed modulus. This value is in excess of the one-percent-of-modulus value predicted by Koehler.⁽¹⁾ Above 600°C pure Mo is stronger than the Cu-Mo laminate, but the Cu-Mo laminate exceeds the rule-of-mixtures predicted strength below 788°C and is nearly equal to it at 987°C.

In general, above 750°C the composite should have electrical properties characteristic of the amount of Cu present (spheroidized structure with a continuous Cu matrix) but mechanical properties approximately equal to an average of Cu and Mo properties. Further, the calculated room temperature tensile strength of a sample heat treated at 1000°C for 4 hours is $\sigma_u = 8798 \text{ kg/cm}^2$ (125,125 lbs/in²). This is approximately 1055 kg/cm² (15,000 lbs/in²) higher than is observed for Mo, almost twice the maximum observed for pure Cu, and 1.4 times the value expected by the rule of mixtures.

Tensile testing to confirm the strength calculations based on hardness data met with only limited success since all fractures were brittle and occurred at low loads, precluding any measurement of σ_u . It was found, however, that composite modulus was $1.53 \times 10^6 \text{ kg/cm}^2$ ($21.7 \times 10^6 \text{ lbs/in}^2$). This was lower than the $2.35 \times 10^6 \text{ kg/cm}^2$ expected from the rule of mixtures and was possibly the result of micro-cracking occurring during pretest fixturing.

Compound-Forming Systems

Lamellar composites of titanium and beryllium-titanium (nominally corresponding to TiBe₁₂) were formed by sputter deposition. The deposits were about 800 square centimeters in area and 0.25 mm thick, and were formed at rates of 0.2-0.3 microns/minute. The polished copper substrates were maintained at 500°C during deposition.

The deposition variables were the thickness of the reinforcing (compound) layer relative to the titanium layer and the repeating thickness of the pairs of layers.

The mechanical properties of the deposits were determined by tensile and three-point bend testing. The tensile strength data was limited by premature failure at strains of less than 10^{-4} . The elastic moduli were 9 to 23% greater than that of titanium, however no correlation with the relative compound or repeating thickness of the layer structure was observed. The observed tensile strengths were in the $2.0-5.3 \times 10^3 \text{ kg/cm}^2$ (29-76,000 lbs/in²) range.

The bend test results revealed the following effects of the repeating unit and relative compound layer thickness:

- a. At equal strain, higher strengths were observed with smaller repeating unit layer thickness and/or higher relative compound layer thickness.
- b. Lower relative compound layer thickness permitted greater plastic strain before fracture, and thus produced the highest observed strengths.

Other property measurements indicated that the intermetallic compound was formed during deposition on the (500°C) substrate, and that the lamellar structure was stable up to 900°C, but broke down into a nonplanar geometry at higher temperatures.

It was concluded that the lamellar composites had demonstrated the potential for high strength. The most profitable area for further investigation appeared to be that of smaller repeating unit layer thickness, and smaller proportions of the relative intermetallic compound.

THIN-LAYERED SYSTEMS

MATERIALS AND PROCEDURES

Deposition

Sputtering targets were fabricated from 99.99% pure electrolytic tough pitch (E.T.P.) copper and 99.95% pure molybdenum. Substrates were rolled OFHC copper, 61.8 cm x 12 cm. Substrates used for initial deposits were 0.051 cm thick and had a surface finish of approximately 0.8 microns. From the rolling operation, they had small grooves oriented parallel to the long dimension of the substrate. Substrates used for later deposits were 0.064 cm thick and had a surface finish of better than 0.2 microns. The properties of the Cu and Mo used as components to form the lamellar composites are listed in Table I.

TABLE I. Properties of the Components of the Lamellar Composite

<u>Property</u>	<u>Cu</u>	<u>Mo</u>
Density (g/cm ³)	8.96	10.2
Melting Point (°C)	1083	2625
Thermal Expansion (/°C)	16.5 x 10 ⁻⁶	4.9 x 10 ⁻⁶
Latent Heat of Fusion (cal/g)	50.6	70
Electrical Resistivity (μ ohm-cm)	1.6730	5.17
Modulus of Elasticity (kg/cm ²)	1.2 x 10 ⁶	3.5 x 10 ⁶
Crystal Structure	fcc	bcc
Lattice Constant = a(kX)	3.6080	3.1400

A diagram of the sputtering apparatus is illustrated in Figure 1. In operation the substrate rotates around the half-cylinder Cu and Mo targets so that a given area on the substrate is exposed to the Cu target for the first half of a revolution and to the Mo target for the second half of the revolution. Deposit layer thickness is determined by substrate-rotation and sputter-deposition rates. In experiments to date the rotation rate has been fixed at 44 rpm. The deposit (substrate) temperature is controlled by contact with a water-cooled substrate holder. Temperature is measured with a thermocouple which penetrates the substrate holder and contacts the Cu substrate.

The sputtering system is typically evacuated with a liquid nitrogen trapped oil diffusion pump to 9×10^{-7} torr for 18 hr before deposition begins. Then high-purity krypton sputtering gas is admitted to the sputtering chamber until a pressure of 3μ is achieved. The Cu substrate is etched by ion bombardment with 100 v Kr^+ ions for approximately 10 min to produce an atomically clean surface. During sputter deposition the voltages applied to the Cu and Mo targets are adjusted independently to obtain the desired sputtering rates. It was found that substrate bias voltage could not be varied effectively in this apparatus. Substrate potential, therefore, was very close to 35 volts (plasma related for floating potential) for all deposits.

The history of deposits made to date is summarized in Table II.

Heat Treatment

Specimens from TLC-4 and OTLC-2 were heat treated for various times at temperatures up to 1000°C in a vacuum furnace capable of 1×10^{-6}

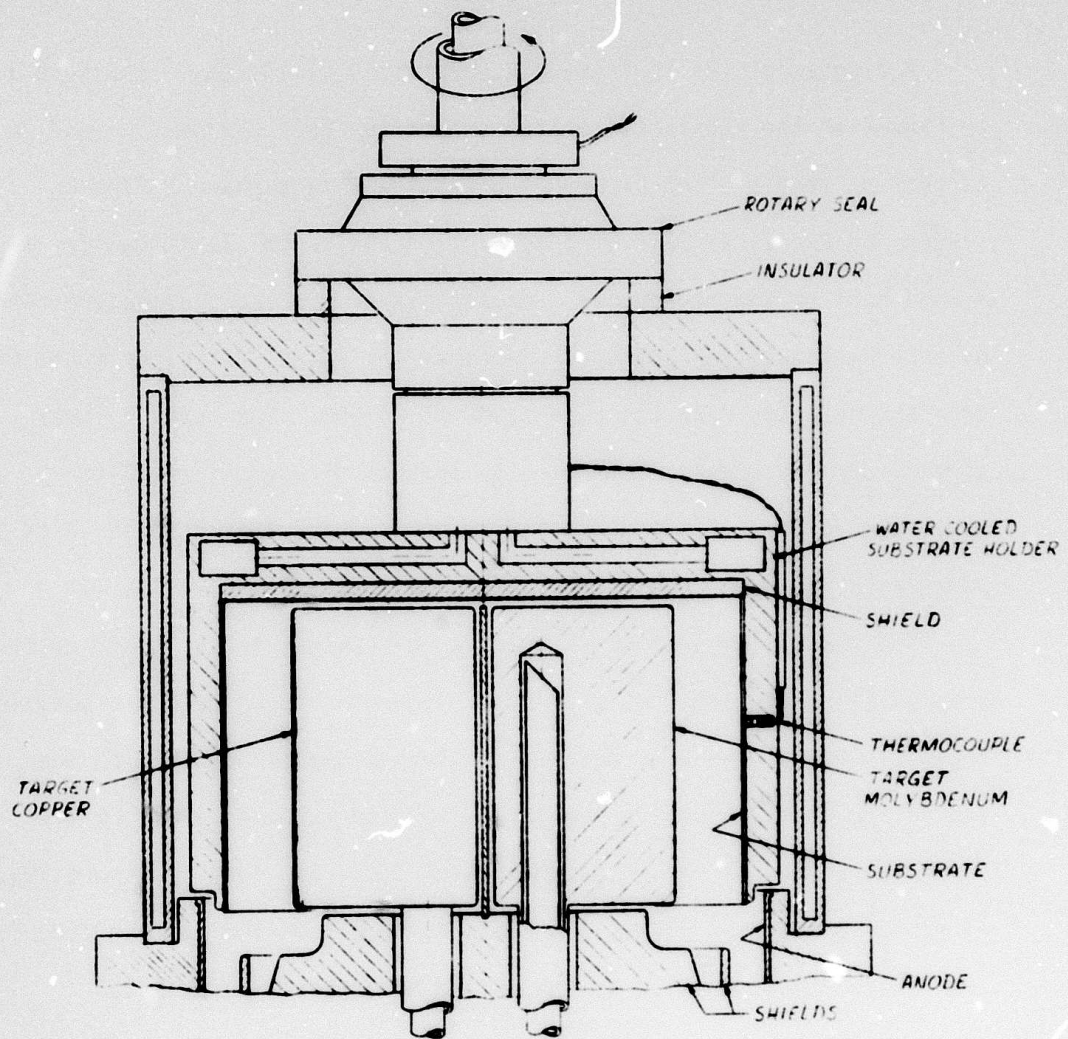


FIGURE 1. Sputtering Hardware for Deposition of Lamellar Composites

TABLE II. Deposition History and Comment

Deposit Number	Substrate Surface	Deposit Thickness (cm)	Temperature (°C)	Approximate Thickness (Å)		Substrate Etched	Deposition Interruption	Deposit Surfaces	Shields	Comments
				Cu	Mo					
OTLC-1	Rough	None	---	---	---	No	---	---	S.S.* & Cu	Faulty assembly
OTLC-2	Rough	0.076	65	50	50	No	Many	Good, some defects	S.S. & Cu; peeling	Electrical problems limited length of run.
OTLC-3	Rough	None	---	---	---	No	---	---	---	Electrical problems terminated run at its startup.
TLC-1	Rough	None	65	---	---	No	---	---	S.S. & Cu; peeling	Shield peeling produced shorts and terminated run.
TLC-2	Rough	0.023	65	50	50	Yes	One after 2 hours	Good, very few defects	S.S. & Cu; peeling	Shield peeling produced shorts and terminated run.
TLC-3	Rough	0.028	450	50	50	Yes	None	Good, few defects	S.S. & Cu; peeling	System vented to air at 450°C; deposit badly oxidized; shield peeling produced shorts and terminated run.
TLC-4	Rough	0.025	95	50	50	Yes	None	Good, few defects	S.S., Cu and Ta; bad peeling	Shield peeling produced shorts and terminated run.
TLC-5	Smooth	0.036	100	95	24	Yes	None	Good, few defects	S.S. & Cu; peeling	Shield peeling produced shorts and terminated run.
TLC-6	Smooth	0.069	400	50	50	Yes	None	Good, few defects	Cu; peeling	Shield peeling produced shorts and terminated run.

*S.S. = 304 stainless steel

torr at 1000°C. In addition, specimens from TLC-2 were heat treated in an evacuated and inert gas back-filled hot hardness testing apparatus. A summary of heat-treatment conditions is given in Table III. Deposits TLC-2 and TLC-4 were chosen for the treatment because of their high quality and deposit OTLC-2 was chosen because it was thick enough for transmission electron microscopy.

TABLE III. Heat-Treatment Parameters for Deposits TLC-4, TLC-2, and OTLC-2

Temperature (°C)	Time (hrs)			
	1	2	3	4
500	TLC-2 TLC-4	TLC-4	OTLC-2	TLC-4
650	TLC-2			
750	TLC-4	OTLC-2 TLC-4	OTLC-2	TLC-4
800	TLC-2			
1000	TLC-4 TLC-2	OTLC-2 TLC-4		OTLC-2 TLC-4

Evaluation

X-Ray Diffraction

Nickel-filtered Cu K_α radiation was used in a flat film Unicam technique and in an x-ray diffractometer with digitized data acquisition and analysis to determine structure of as-sputtered and heat-treated specimens. Specimens were examined with the x-ray beam arriving perpendicular to the layer planes. Fifty percent of the x-ray intensity is produced by the first 15,400 Å of the surface. This provides sufficient x-ray penetration to examine on the order of 300 layers and pseudomorphic regions simultaneously.

Transmission Electron Microscopy

A thinning technique has been developed for Cu-Mo laminates that allows the use of a 200-kV electron microscope to examine layer structure. This technique is being used to examine deposits parallel to the layer planes. Transmission foils are only as wide as the deposit thickness, then, so deposit thickness of at least 0.051 cm was required.

Hardness Testing

Microhardness of deposits is being measured at room temperature in both as-deposited and heat-treated conditions. In addition, hot hardness is being measured, by Professor John Moteff at the University of Cincinnati, as a function of time at temperatures to 1000°C. An inert-atmosphere cantilever-beam-loading apparatus is used for this work. Diamond pyramid indentors and loads of 500 grams or less are being employed. Hardness results are being used to estimate tensile properties for a wide range of conditions.

Tensile Testing

ASTM E8 subsize specimens are being fabricated from the deposits with a Tensilgrind machine. The Cu substrate is machined from the deposit in the 0.625 cm x 2.54 cm gauge length which is then polished. Strain gauges are cemented to both sides of its length. Tensile tests are performed at room temperature in an Instron Model TTC tensile testing machine.

Fracture surfaces are being examined in a scanning electron microscope to determine mode of fracture and its relation to composite structure.

Other Techniques

Auger electron spectroscopic analysis was performed by Professor Gotfried Wehner at the University of Minnesota on as-deposited specimens and specimens heat treated for various times at temperatures to 1000°C. No useful information was obtained.

Stored energy release investigations are being carried out in a Perkin-Elmer DSC-2 scanning calorimeter with a maximum temperature capability of 725°C. Information obtained from these investigations should allow prediction of annealing mechanisms and activation energies and, therefore, prediction of mechanical behavior for extended times at elevated temperatures. Data is not yet available.

Resistivity measurements are being made in a Battelle-Northwest designed and constructed apparatus using a four-probe technique and a digital data acquisition and analysis system. Only preliminary data is available to date. Objectives are the same as for the calorimetric investigation described above. The preliminary data indicates that the existing BNW resistivity techniques will be adequate for these purposes.

RESULTS AND DISCUSSION

Deposition

Shield peeling has been a problem in all depositions. Various precautions were taken to enhance adherence between sputtered material and shields. These included cleaning the shields in various solvents and bead blasting, machining, and vacuum baking them before deposition. Different shielding materials (stainless steel, tantalum, and OFHC copper) were tried and evaluated as a possible solution. OFHC copper

was found to be the most satisfactory. Peeling was successfully eliminated in all areas except on shields near the filament.

Deposits made at 65 and 95°C were very highly stressed. When they were removed from the cylindrical substrate holder, these substrates straightened out in the 61.8-cm dimension (the cylinder circumference) and warped approximately 1 cm in the 12-cm dimension (parallel to the cylinder axis) towards the deposit. This behavior is illustrated in Figure 2. Deposits made at 400 and 450°C retained the shape of the cylindrical substrate holder.

Evaluation

X-Ray Diffraction

Low temperature deposits examined to date were heavily textured with (111) Cu and (110) Mo planes oriented parallel to the deposit-substrate interface. The only high temperature deposit which has been examined (TLC-3) was heavily textured in the Mo layers with (110) Mo planes oriented parallel to the deposit-substrate interface. The Cu layers were slightly textured with (100) Cu planes oriented parallel to the deposit-substrate interface. This corresponds to a recrystallization texture previously observed in sputtered Cu.⁽⁵⁾ No evidence of structure other than fcc Cu and bcc Mo has been observed.

Peak splitting or extra lines were observed in samples in the as-deposited condition when the sputter deposition temperature was below 100°C, Figure 3. Similar diffractometer traces have been observed at this laboratory in instances when intensity was very high, and were found to be a phenomenon related to the x-ray detection electronics. To demonstrate that this phenomenon was not responsible for the peak

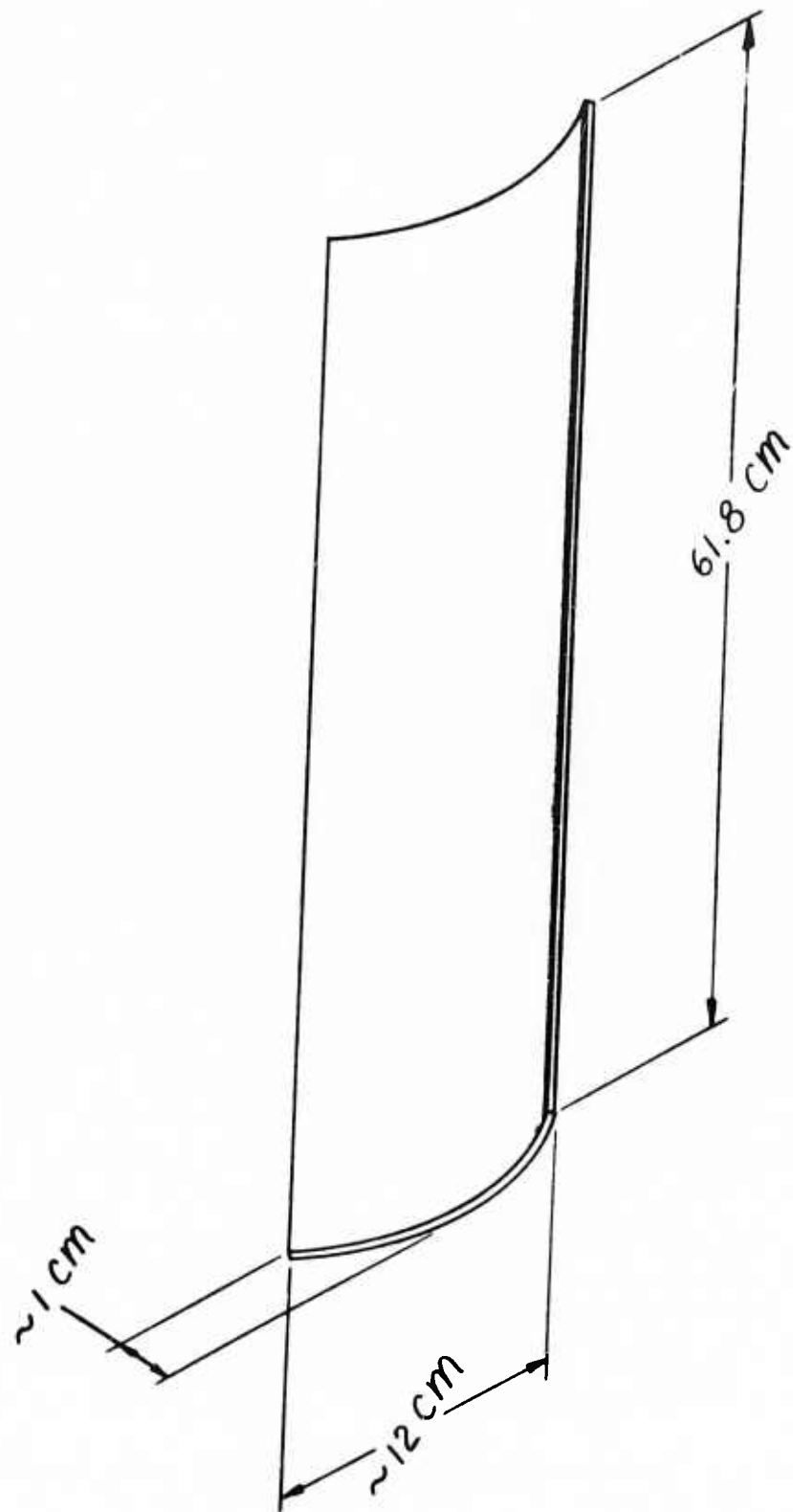
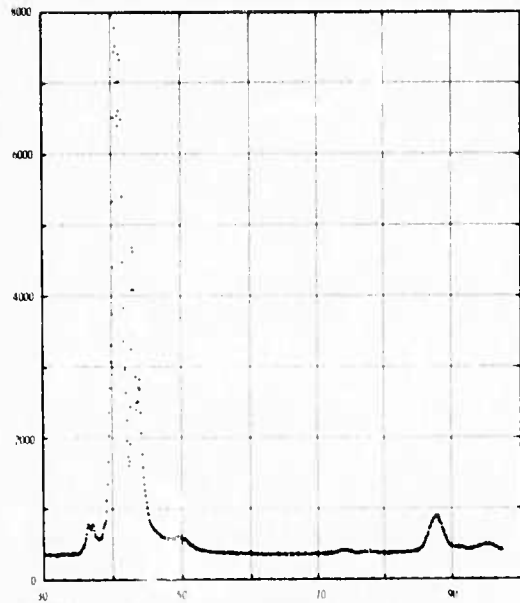
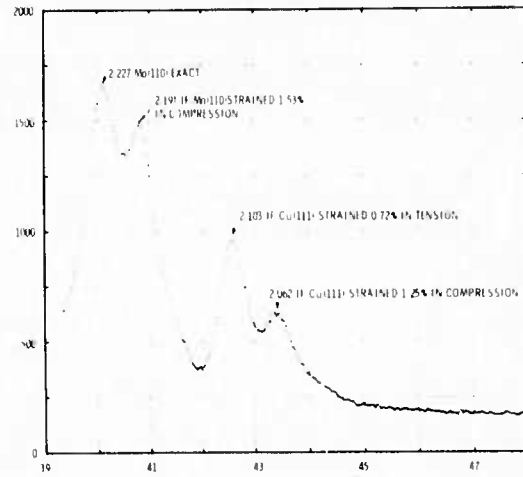


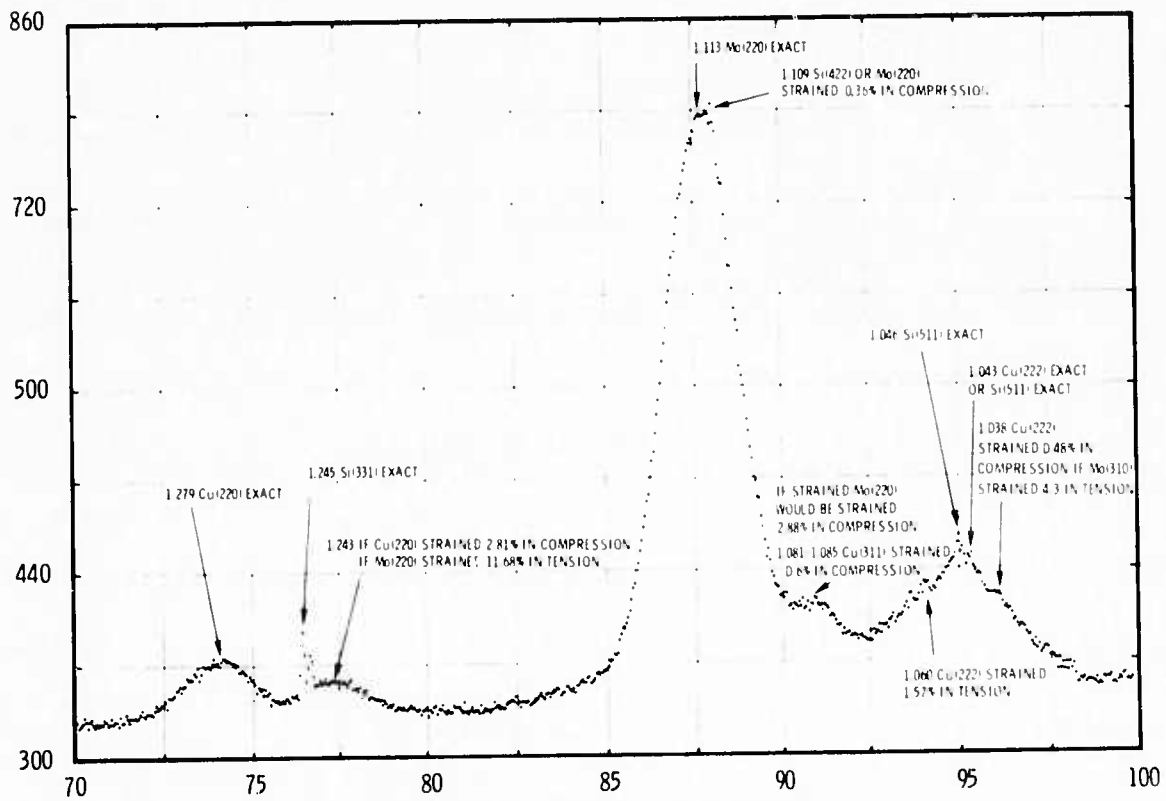
FIGURE 2. Approximate Configuration of 65 and 95°C Deposits
After Removal from the Substrate Holder



a) Condensed Pattern



b) Low Angle Region, Expanded



c) High Angle Region, Expanded

FIGURE 3. Diffractometer Patterns of OTLC-2, As Sputtered.

splitting observed, a Unicam film technique was used to record an x-ray pattern from a sample displaying extra or split peaks in the diffractometer. The presence of the peak splitting or additional peaks in this film pattern, illustrated in Figure 4, conclusively shows that the lines observed with the diffractometer were not due to instrumental factors.

The step scanning diffractometer technique used to obtain Figure 3 was developed in order to gain more detailed insight into the structure of the lamellar composites. In this technique, the diffractometer was used to measure x-ray intensity as a function of θ in a step-wise rather than continuous manner, with the diffractometer remaining stationary and counting at each incremental value of θ for a predetermined length of time. Peak locations were verified by comparison with a Si pattern superimposed on the Cu-Mo pattern by dusting the laminate surface with annealed Si powder prior to the recording of the x-ray diffraction pattern. X-ray intensity data was digitally recorded. A computer program was written to analyze and expand the data into the forms illustrated in Figures 3b and c. Since it is possible that lattice strain, caused by Cu in the Mo lattice and vice versa, is responsible for the positions of the observed diffraction lines, diffractometer patterns will be recorded on the same sample at a variety of temperatures from approximately -195°C to $+100^{\circ}\text{C}$ in an attempt to verify this consideration. Comparison of line positions and amplitudes should clarify the nature of the Cu-Mo interface region and allow qualitative prediction of the effect of Cu-Mo mixing at the interfaces and resulting mechanical property effects.

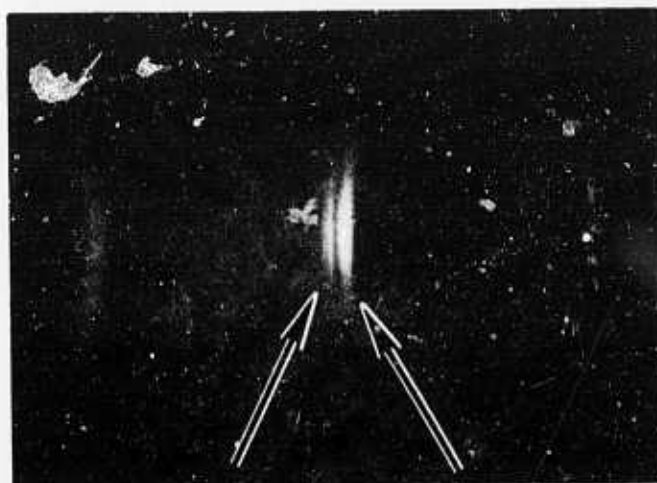
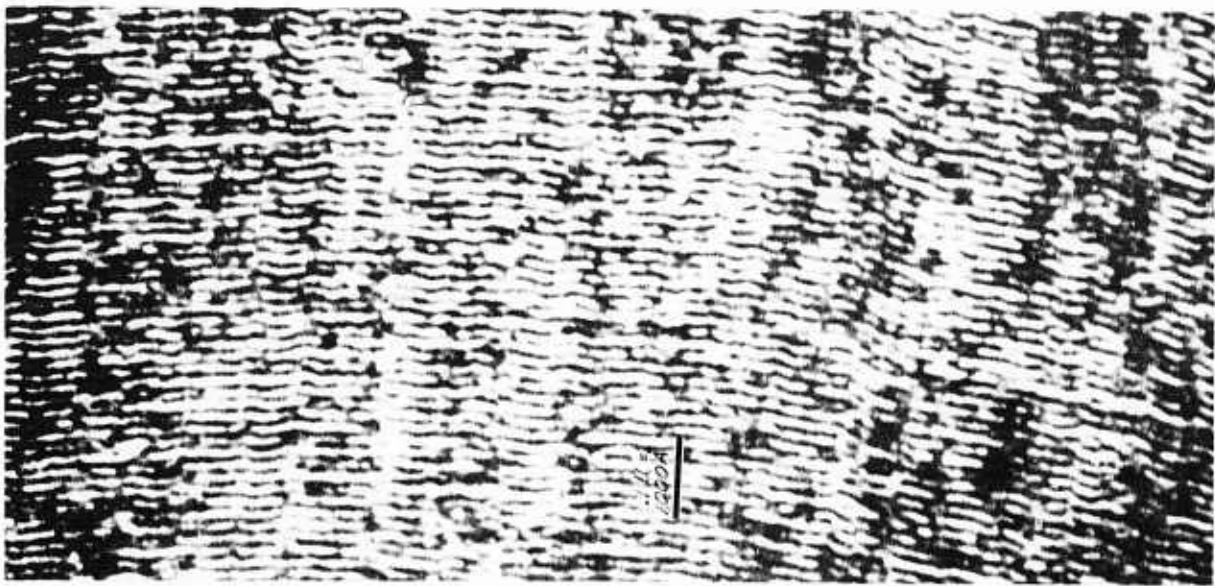


FIGURE 4. Unicam X-Ray Diffraction Pattern of OTLC-2, As-Sputtered. Note (111) Cu (left arrow) and (110) Mo (right arrow) Peak Splitting.

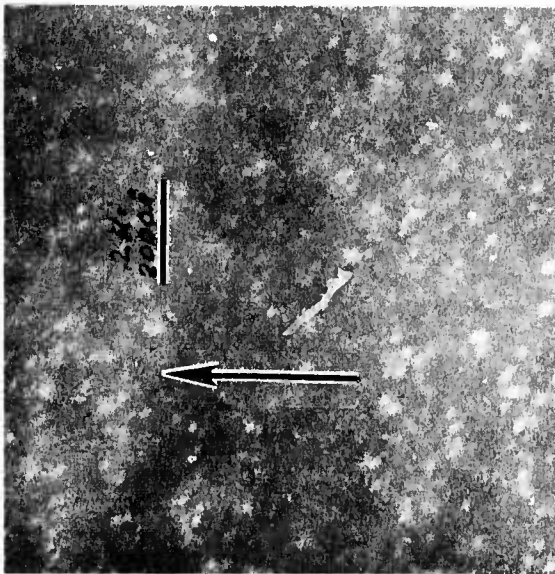
Transmission Electron Microscopy

Transmission electron microscopy (TEM) in earlier work⁽⁶⁾ showed that a structure consisting of layers on the order of 50-100 Å thick had been achieved and, further, that these layers were very uniform and continuous. Thinning techniques have been further developed to show this structure in more detail, and these techniques have been applied to Cu-Mo thin laminate samples that were heat treated at temperatures to 1000°C for times from 2 to 4 hours. It was found that the thin layered structure persists after 3 hours at 500°C, Figure 5a. In addition, dark field TEM of the 500°C-3 hr sample, Figure 5b, which is also representative of the as-sputtered material, revealed equiaxed 50-100 Å diameter grains that are approximately randomly oriented about an axis perpendicular to the substrate-deposit interface i.e., perpendicular to the layer plane. Figure 5c is an electron diffraction pattern of the same region shown in Figures 5a and 5b. The presence of both Mo and Cu diffraction lines indicates that both metals are still present in the thinned foil.

Four hours at 1000°C resulted in a breakdown of the layered structure by spheroidization of the Mo, Figure 6a. The spheroidized structure consists of Mo spheres in a twinned Cu matrix with the Mo spheres growing in diameter with increasing temperature and with increasing time at temperature, Table IV. Figure 6b seems to indicate that coarsening of the Mo spheres proceeds, in the later stages by coalescence. Figure 6c shows the presence of both Cu and Mo rings in the electron diffraction pattern.



a) Layer Thickness of Approximately 80 \AA . Structure is Apparently Unchanged from the As-Deposited Condition. 100,000X

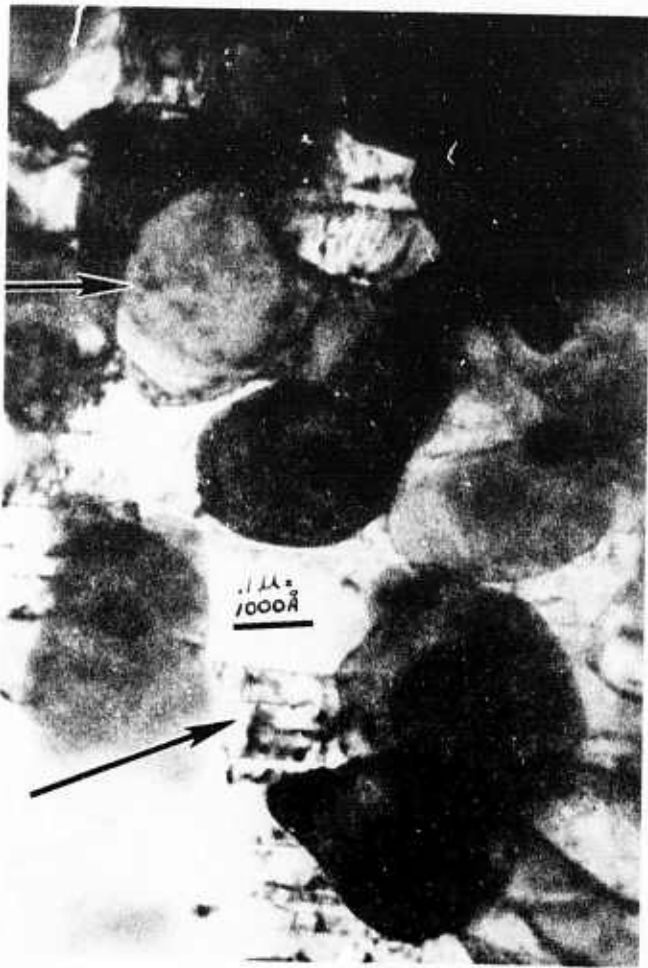


b) Dark Field Using First Mo Diffraction Ring. Same Region as Above. Layers are Parallel to the Arrow. Note Apparent Equiaxed Grains $50\text{-}80 \text{ \AA}$ in Diameter. 51,000X

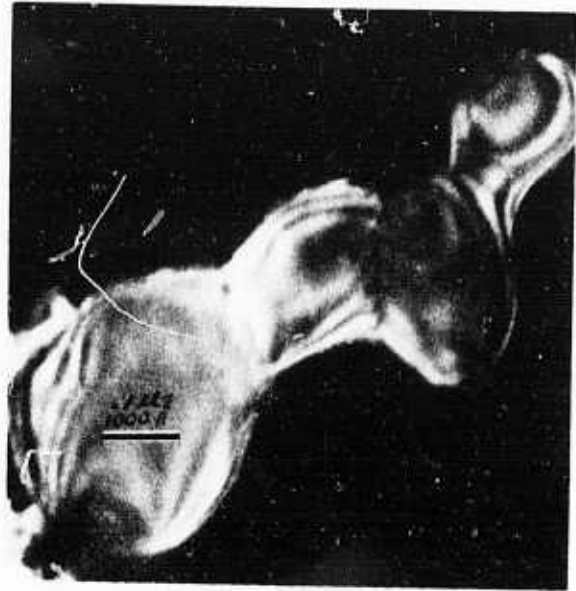


c) Electron Diffraction Pattern. Both Cu and Mo Rings are Visible.

FIGURE 5. TEM Micrographs of OTLC-2, Heat Treated at 500°C for 3 Hours. Viewed Parallel to Layer Planes.



a) Mo Spheres (top arrow) in a Twinned Cu Matrix (bottom arrow). 101,000X



b) Dark Field Micrograph Using the First Mo Ring Shows Structure of Mo Sphere During Coalescence. 101,000X



c) Electron Diffraction Pattern. Both Cu and Mo Rings are Visible.

FIGURE 6. TEM Micrographs of OTLC-2, Heat Treated at 1000°C for 4 hrs. Viewed Parallel to Prior Layer Planes.

TABLE IV. Influence of Heat Treatment on Microstructure of Deposit OTLC-2.

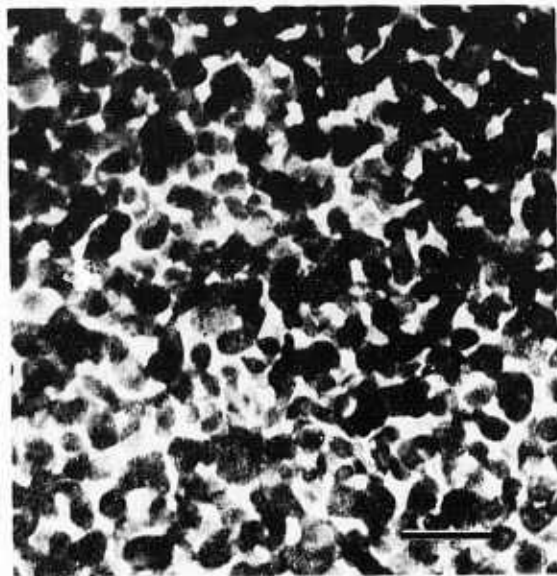
Heat Treatment Temperature (°C)	Time (hrs)	Microstructure	Approximate Mean Layer Thickness or Sphere Diameter, Å	Figure Illustrating Structure
500	3	Layered	80	5a
750	2	Spheroidized	860	7a
1000	2	Spheroidized	2130	8
1000	4	Spheroidized	3000	6a

Figures 7 and 8 illustrate the effect of intermediate anneals at 750°C for 2 hrs and 1000°C for 2 hrs respectively. Because of control difficulties, however, thinning resulted in nearly complete removal of Cu in the 750°C-2 hr and 1000°C-2 hr samples as illustrated in the electron diffraction pattern in Figure 7b.

Hardness Testing

Room Temperature Hardness

Room temperature hardness was measured on samples in both as-sputtered and heat treated conditions. Preliminary measurements on polished surfaces of as-sputtered samples indicated that hardness was the same whether measured parallel to the plane of the substrate surface (layer plane) or perpendicular to this plane. This was taken to be an indication of isotropic mechanical properties. Results of subsequent room temperature hardness testing are summarized in Table V. In addition, Figures 9 and 10 illustrate hardness changes as a function of time and temperature, respectively. Note that some hardness data was obtained on as-sputtered surfaces while other data was obtained on polished surfaces.



a) Note that the Layered Structure is no Longer Present. Mo Spheres are Approximately 860 Å in Diameter. 51,000X



b) Electron Diffraction Pattern. Only Mo Rings are Visible.

FIGURE 7. TEM Micrographs of OTLC-2, Heat Treated at 750°C for 2 hours. Viewed Parallel to Prior Layer Planes.

FIGURE 8. TEM Micrograph of OTLC-2 Heat Treated at 1000°C for 2 hrs. Viewed Parallel to Prior Layer Planes. Mo Spheres are Approximately 2130 Å in Diameter. 94,000X



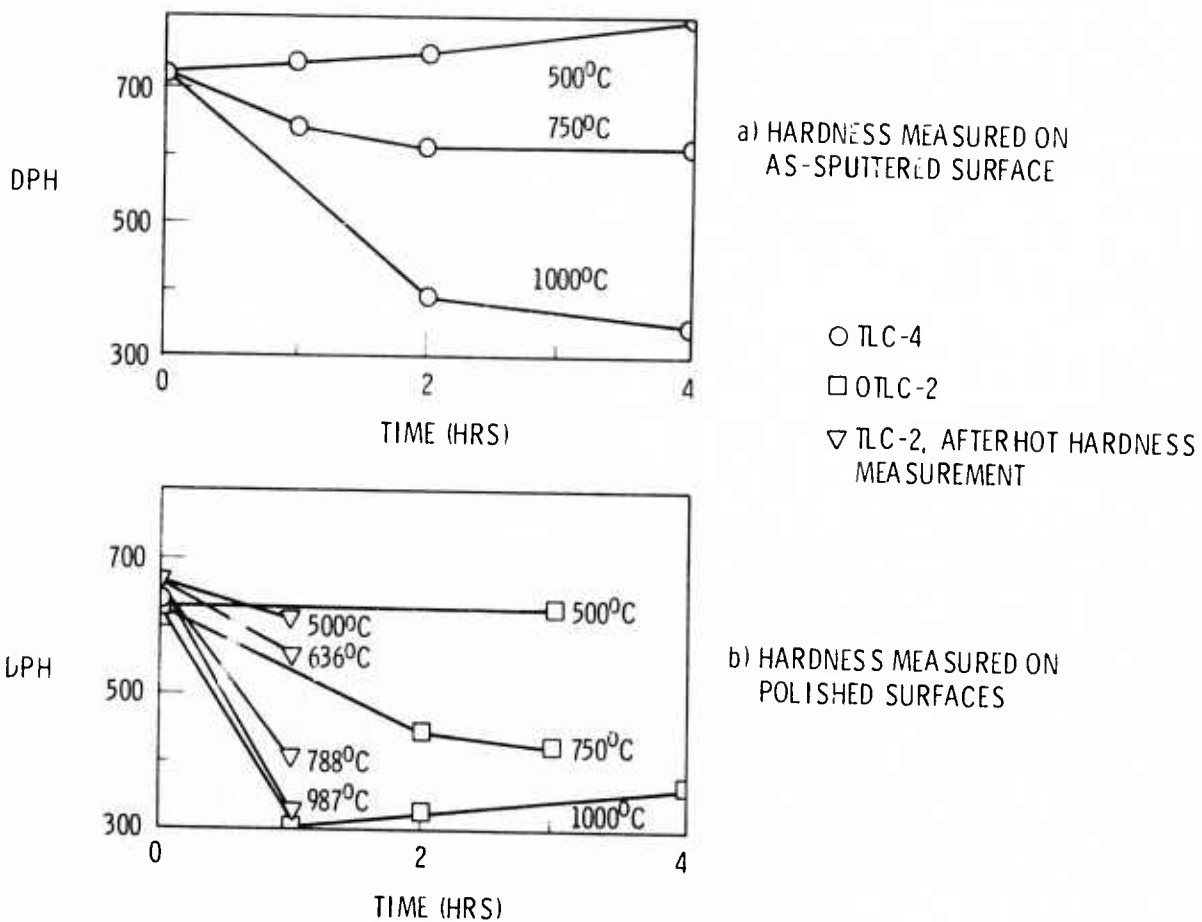


FIGURE 9. Room Temperature DPH Versus Time at Heat Treating Temperature.

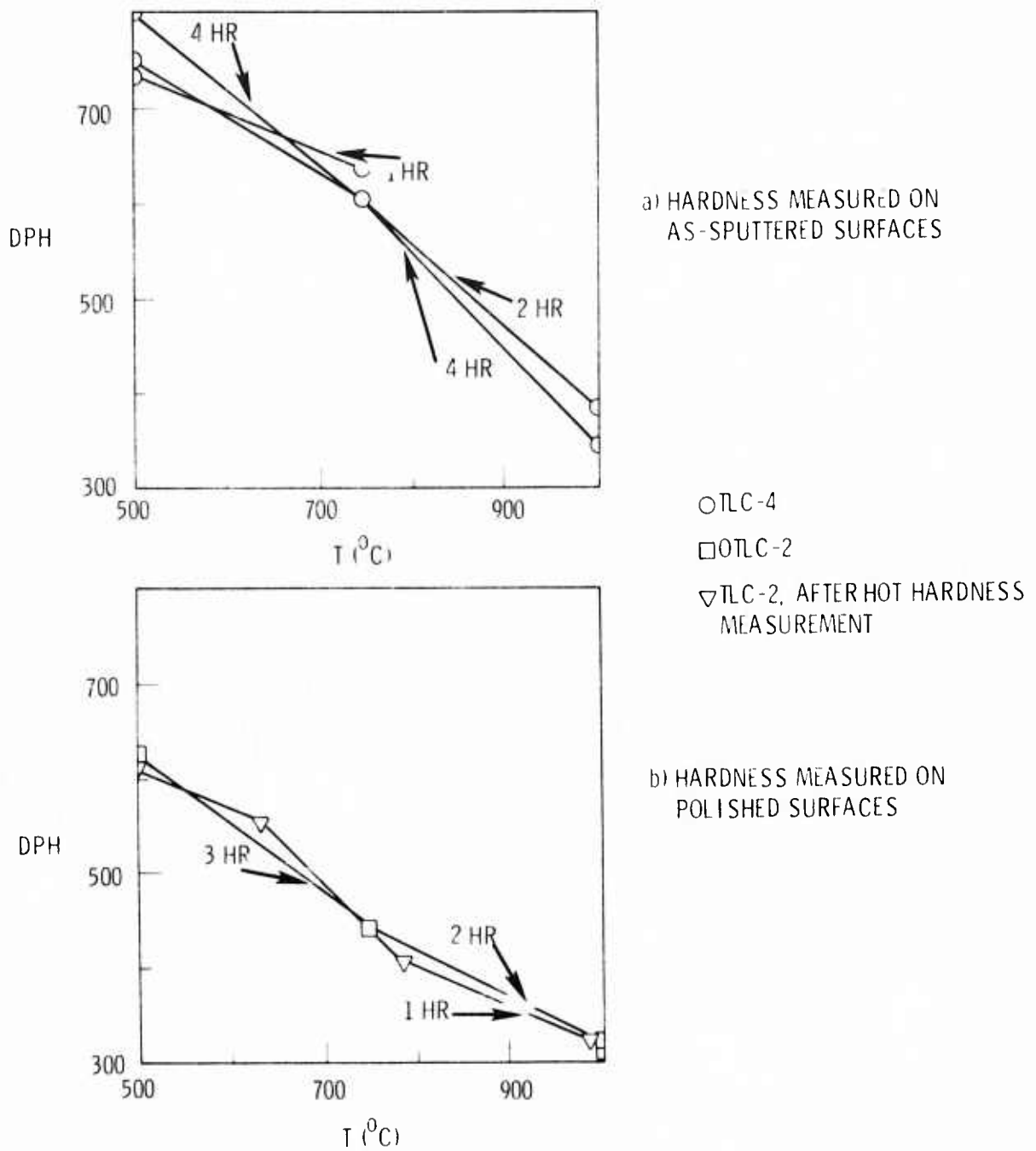


FIGURE 10. Room Temperature DPH Versus Heat Treating Temperature for Several Heat Treating Times.

TABLE V. Room Temperature DPH Hardness Measurements

Deposit	Heat Treatment Temperature (°C)	(No Heat Treatment)	Time at Temperature (hrs)			
			1	2	3	4
TLC-4	500	717*	731*	743*		801*
	750	636**	639*	603*		605*
	1000			383*		341*
OTLC-2	500	630**				623**
	750			446**	426**	
	1000		304**	328**		370**
TLC-2	500	669**	612**			
	636		554**			
	788		408**			
	987		325**			

*Hardness was measured on as-sputtered surface

**Hardness measured on metallographically polished surface.

Hardnesses for as-sputtered surfaces were approximately 80 DPH higher than for polished surfaces, in the as-sputtered condition.

While incomplete at this time, the data presented in the figures indicate several possible conclusions. No structural change as indicated by hardness of TLC-4 and OTLC-2 (Figure 9) was observed for times less than 3 hours at 500°C. Variations in the hardness of TLC-2 were not considered significant because of the heat treating procedure used for it. It is possible that some hardening occurred after 4 hours at 500°C (TLC-4, Figure 9a) but more data would be required to verify this. Softening, presumably indicating structural changes, was observed after one hour at temperatures of 636°C and above (TLC-2, Figure 9b). This softening proceeded more rapidly with increasing temperature (Figs. 9a,b).

In addition, the minimum hardness reached at a given heat treatment temperature decreased with increasing temperature (Figures 9a, b). The minimum hardness observed after the most severe heat treatment (4 hrs at 1000°C) was still greater than the 300 VHN observed for rolled Mo bar material.

These results agree well with the TEM results. It seems probable that the softening phenomenon is associated with breakdown of the laminate structure by Mo spheroidization. Further, it is expected that hardness of the spheroidized structure is related to Mo sphere size and spacing through the resistance to dislocation movement offered by the Mo spheres.

Hot Hardness

Hot hardness was measured on polished surfaces of deposit TLC-2 using a diamond indenter, cantilever loading, and an evacuated and inert gas flushed system.⁽⁷⁾ The test results are presented in Table VI. Since there was no apparent influence of time at temperature on hardness the data could be averaged. Further it was decided to group the results for all three indenter loads and average them in spite of the fact that no explanation can be given for the influence of indenter load on hardness at 636°C. Note also that the initial hardness decrease was not monitored because approximately one hour was required to reach test temperature.

TABLE VI. Influence of Temperature on Hot Hardness of TLC-2

Test Temperature T, °C	Time at Temperature t, min	VICKERS HARDNESS NUMBER		
		100 gm load	200 gm load	500 gm load
636	0	127.7		
	5	137.5		
	6		146.3	
	7			164.6
	15	139.3		
	16		149.0	
	30	134.1		
	31		142.4	
	60	137.5		
	61		149.0	
	62			163.6
			AVERAGE = 144	
788	0	64.6		
	1		69.2	
	2			73.9
	5	69.3		
	6		72.8	
	7			75.1
	15	63.0		
	16		68.8	
	30	60.9		
	31		69.6	
	60	68.7		
	61		67.5	
62			68.4	
		AVERAGE = 67		
987	1		18.6	
	2			15.2
	5	17.6		
	6		17.9	
	7			15.8
	15	17.0		
	16		18.3	
	30	18.0		
	31		19.3	
	60	18.3		
	61		20.0	
	62			14.7
		AVERAGE = 18		

Calculation of Ultimate Tensile Strength from Hot Hardness

If it is assumed that the Cu-Mo material does not strain harden, then it may be reasonable to develop an ultimate strength-hardness relationship for this material similar to the relationship $\sigma_u(\text{lbs/in}^2) = 515 (\text{BHN})$ which is commonly used for steels.⁽⁸⁾ Published⁽⁹⁾ VHN vs tensile strength data for Mo was used to arrive at a constant of proportionality of $\frac{\sigma_u}{\text{VHN}} = 385$ for the Cu-Mo laminate. Since Mo has very little ductility at room temperature and since work-hardening tendencies of Cu would tend to increase the value of $\frac{\sigma_u}{\text{VHN}}$, this value is expected to be conservative.

Ultimate tensile strengths calculated using this constant and measured hot hardnesses for the Cu-Mo laminate structure are presented in Table VII, along with published ultimate tensile strengths of Cu, Mo, and Cu-2% ThO₂. It can be seen that, at room temperature, the Cu-Mo laminate is much stronger than either pure Cu or pure Mo and is roughly three times stronger than expected by the rule-of-mixtures. Above 600°C pure Mo is stronger than the Cu-Mo laminate. The Cu-Mo laminate however, exceeds the rule-of-mixtures predicted strengths below 788°C and is nearly equal to it at 987°C. This is particularly interesting since above 750°C the structure is no longer a laminate but is composed of discontinuous Mo spheres in a continuous Cu matrix. Above 750°C, then, the composites should have electrical properties characteristic of the amount of Cu present but mechanical properties equal to an average of

TABLE VII. Elevated Temperature Ultimate Tensile Strengths (σ_u) of Cu-Mo Laminate, Cu, Mo, and Cu-2%TiO₂

Temp (°C)	V _H **	Calculated σ_u for Cu-Mo Laminate		Rule-of-Mixtures σ_u Expected for a 50% Cu-50% Mo Composite**		Published σ_u for Cu		Published σ_u for Mo		Published σ_u for Cu-2%TiO ₂ (10) (60 mil wire = .21 cm ² wire)	
		Kg/cm ²	lbs/in ²	Kg/cm ²	lbs/in ²	Kg/cm ²	lbs/in ²	Kg/cm ²	lbs/in ²	Kg/cm ²	lbs/in ²
23	669	18,109	257,565	6,081	86,472	4,429	63,000 ⁽⁹⁾	7,734	110,000 ⁽¹¹⁾	4,106	58,400
636	144	3,898	55,440	2,614	37,171	334	5,600 ⁽¹⁰⁾	4,894	69,600 ⁽¹³⁾	2,088	29,700
782	67	1,813	25,795	2,038	28,980	210	3,000 ⁽¹¹⁾	3,867	55,000 ⁽¹³⁾		
927	12	427	6,930	569	8,091	84	1,200 ⁽¹¹⁾	1,055	15,000 ⁽¹³⁾		

* Specimen TLC-2

** Not Corrected for Crystallographic Texture

Cu and Mo properties. Furthermore, if room temperature hardness of samples heat treated at 1000°C (Table V) is used in this manner to calculate the minimum expected room temperature ultimate tensile strength of the spheroidized structure, the result is $\sigma_u = 8798 \text{ kg/cm}^2$ (125,125 lbs/in²). This strength is 1055 kg/cm² (15,000 lbs/in²) higher than the maximum room temperature ultimate tensile strength of Mo, and 1.4 times the value expected by the rule-of-mixtures.

Tensile Properties

As was reported earlier,⁽⁶⁾ the modulus of TLC-5 was $1.2 \times 10^6 \text{ kg/cm}^2$ ($17.1 \times 10^6 \text{ lbs/in}^2$), which is typical of pure Cu. TLC-5 was deposited at 400°C with thicker Cu layers than Mo layers, so this result was not unexpected. Brittle fractures in TLC-5, however, indicated that brittle fracture was to be expected in lower temperature deposits.

Specimens of deposit TLC-2, sputtered at 65°C, were tensile tested and results were taken as representative of 50-100 Å equal layered deposits made at temperatures near 100°C. An average of four samples produced a modulus of $1.53 \times 10^6 \text{ kg/cm}^2$ ($21.7 \times 10^6 \text{ lbs/in}^2$). The difference between high and low values was $0.253 \times 10^6 \text{ kg/cm}^2$ ($3.6 \times 10^6 \text{ lbs/in}^2$) or 16.6%. One possible cause of the high scatter may be cracking introduced in the specimen during assembly and alignment of the tensile testing apparatus. Cracking may also account for observed average modulus being much lower than the $2.35 \times 10^6 \text{ kg/cm}^2$ ($33 \times 10^6 \text{ lbs/in}^2$) predicted by rule-of-mixtures modulus values calculated using stiffness and compliance constants tabulated by Tegart⁽¹⁴⁾ to correct for crystallographic orientation of the layers.

In all cases fractures were brittle, as expected. Failure also occurred at low loads, primarily because of the well known difficulties associated with the uniaxial tensile testing of brittle materials. Because of the brittle behavior, then, it was not possible to determine yield strengths or YS/elastic modulus ratios. It is expected that this elastic-only behavior would persist until individual layer thickness in a layered structure or Mo sphere spacing in a spheroidized structure became large enough to allow significant dislocation motion. This dimension would probably be on the order of 2000 Å. If this were the case, then plastic deformation would not be observed in 50-100 Å-thick-layered structures of Cu and Mo for temperatures less than 500°C or for times less than 2 hours at 750°C. Some plastic deformation might be observed in samples heated to 1000°C for 2-4 hours, based on Mo sphere size and separation observed by TEM.

Scanning Electron Microscopy

Scanning electron microscopy of the fracture surfaces was not available at the time of writing.

COMPOUND FORMING SYSTEMS

MATERIALS AND PROCEDURES

In the previous reporting period, the titanium-beryllium system had been selected for investigation. It was intended to examine deposits consisting of alternate layers of metal and intermetallic compound. Since previous work indicated that some difficulty would be encountered in forming the compound layers by in situ reaction of the elemental layers, a sputtering target was designed to deposit the

composition corresponding to the compound directly. This target consisted of a beryllium semicylinder with embedded titanium strips, Fig. 11. The exposed area of titanium was based on sputtering yield data obtained earlier in this program.

Sputtering targets of the pure elements were also fabricated to provide a capability of depositing lamellar composites of Ti + BeTi and Be + BeTi. It was also intended to deposit Ti + Be for use as a control sample to evaluate the effects of the intermetallic compound.

Severe difficulties were encountered in all deposition attempts in which the pure beryllium target was used. The difficulties consisted of flaking of the stray deposit from shields in the apparatus, resulting in electrical short circuits. Several attempts to improve the adherence of the stray deposit were unsuccessful. A decision was made to confine the balance of the year's effort to the Ti + BeTi configuration, which did not experience the flaking problem.

Four Ti + BeTi depositions were utilized to examine the variables of repeating and relative compound layer thickness. Repeating layer thickness gives the total thickness of the repeating unit, metal layer plus compound layer, and was controlled by the rotation rate of the substrate. Relative compound layer thickness was the compound layer fraction of the repeating unit and was controlled by the ratio of the voltages applied to the two targets. Other deposition parameters were maintained essentially constant. The polished copper substrate was electrically floating and its temperature was held at 500°C.

The calculated values of the repeating and relative compound layer thickness for the four deposits are shown in Table VIII.

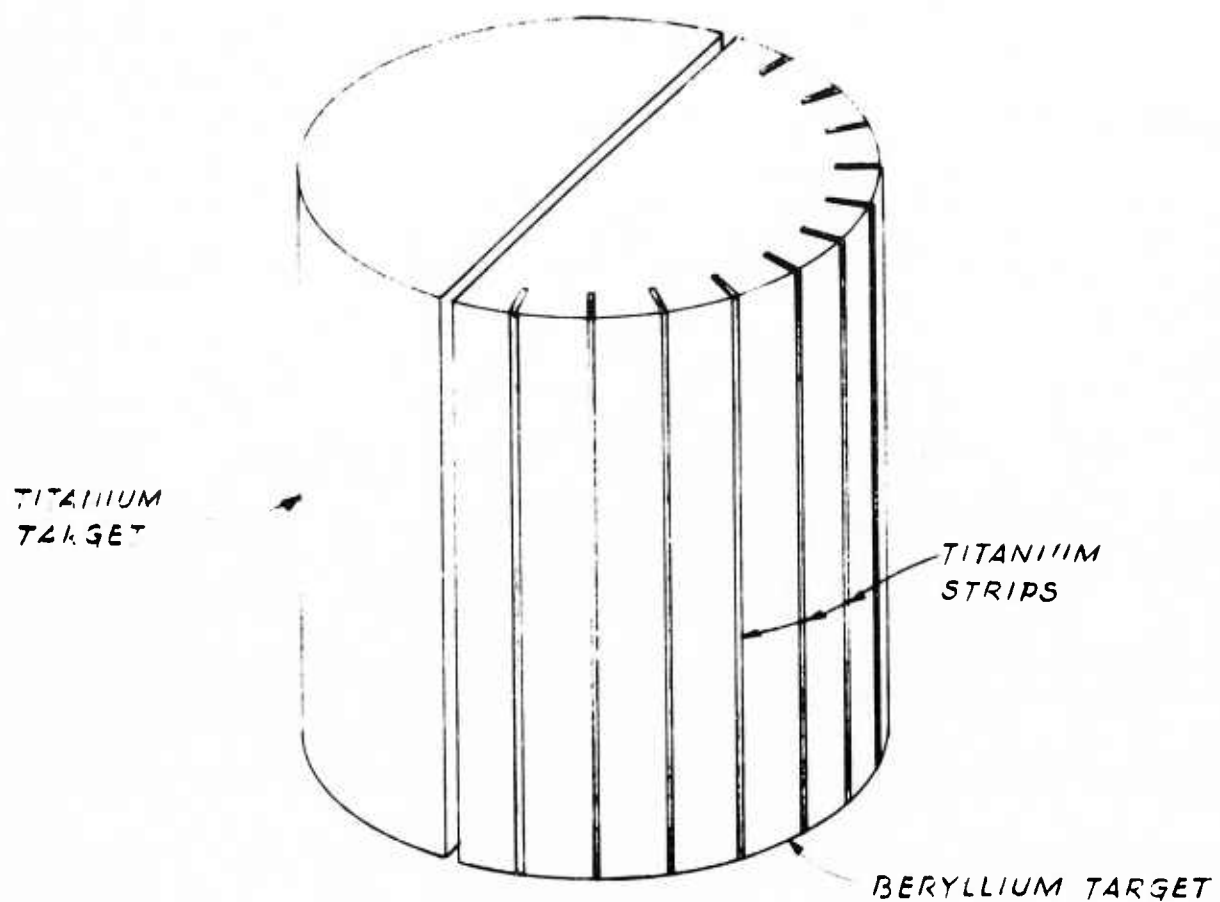


FIGURE 11. Arrangement of Sputtering Targets for the Deposition of Ti + BeTi Lamellar Composites. The Titanium and Beryllium Targets are Electrically Independent; the Substrate is Concentric with the Targets and Rotates.

TABLE VIII. Calculated Characteristics of
Ti-BeTi Lamellar Composites

<u>Deposit</u>	<u>Repeating Layer Thickness</u> <u>Microns</u>	<u>Relative Compound</u> <u>Layer Thickness</u> <u>(%)</u>
24/0.2	0.23	24
14/0.2	0.20	14
14/0.1	0.10	14
24/0.1	0.12	24

It should be noted that the titanium layers in deposits 24/0.2 and 14/0.1 were the same thickness, as were those in deposits 14/0.1 and 24/0.1. The change in repeating layer thickness was due to the change in the thickness of the compound layer.

The deposits were about 800 cm^2 in area and 0.25 mm thick, and were deposited at a rate of 0.2-0.3 microns/min. The deposits were sectioned into blanks for miniature tensile specimens, which were shaped in a beryllium-adapted Tensilgrind machine. Specimens were tested in the as-deposited condition and after heat treatment. Since all specimens failed in a brittle manner, usually at or near the grips, three point bend tests were resorted to. Fracture surfaces were examined in the scanning electron microscope.

In an attempt to determine the processes occurring during heat treatment, the electrical resistivity was monitored as a function of time after upquenching specimens into a fluidized bed maintained at the heat treatment temperature.

RESULTS AND DISCUSSION

Deposit Quality

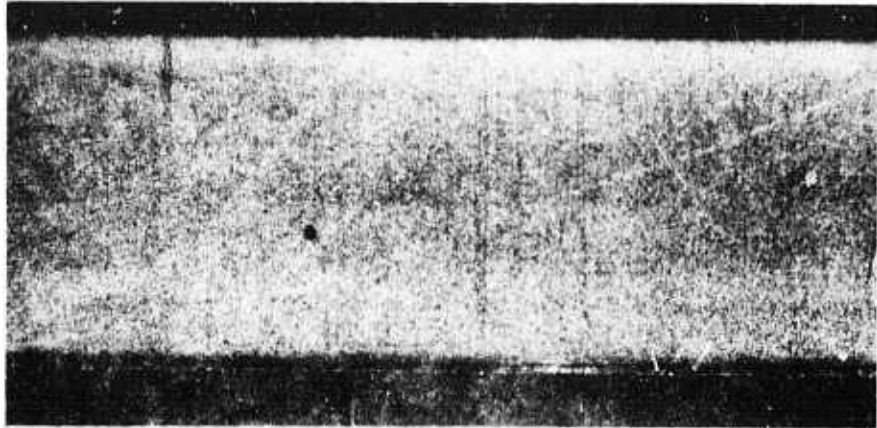
All four deposits were of generally excellent surface finish. Very few growth defects of the "wart" or nodule type commonly observed in deposited materials were present. This may be due to either or both of two factors: the continual interruption of the deposition process inherent in forming a lamellar composite; and the geometry of the target-substrate pair, which restricted the angle of incidence at which condensing material arrived at the substrate. The only visible defects were areas where random flakes had landed on the instantaneous deposit surface and stuck long enough to be bonded by the condensing sputtered material. A typical deposit cross section is shown in Figure 12a. The lamellar structure is shown in Figure 12b. The layer thicknesses correspond well with the values calculated from the sputtering yields of the respective materials, Table VIII.

Mechanical Properties

Tensile

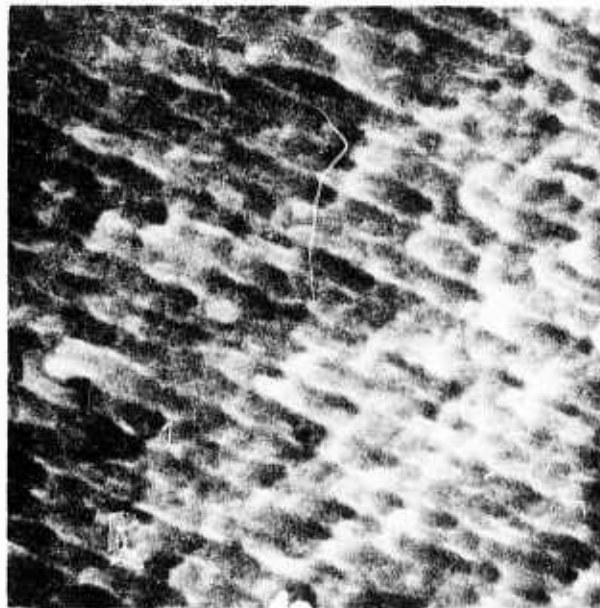
The tensile properties of the lamellar composites in the as-deposited condition are presented in Table IX.

Growth
Direction



a) Optical Micrograph, 100X

Growth
Direction



b) Scanning Electron Micrograph,
Showing Lamellar Structure, 15,000X

FIGURE 12. Cross Section of Typical Lamellar Composite.

TABLE IX. Tensile Properties of Lamellar Composites

Deposit	Elastic Modulus		Ultimate Tensile Strength	
	10^6 kg/cm ²	10^6 psi	10^3 kg/cm ²	10^3 psi
24/0.2	1.25	17.92	2.04	29.4
	1.34	19.21	4.04	58.1
	1.35	19.37	2.59	37.2
14/0.2	1.31	18.90	3.72	53.5
	1.43	20.62	4.37	62.9
	1.30	18.68	4.30	61.8
14/0.1	1.41	20.28	4.37	62.9
	1.32	19.00	4.02	57.9
	1.33	19.13	5.30	76.3

All samples failed in a brittle manner at a plastic strain of less than 10^{-4} , therefore the strength values are more indicative of the flaws present (or the material's sensitivity to such flaws) than the actual material strength. The measured strengths were in the $2.0-5.3 \times 10^3$ kg/cm² (29-76,000 psi) range. The elastic moduli are all higher than that of titanium, indicating that some reinforcement has been obtained. The moduli, however, are not proportional to the percentage of compound and are significantly less than those predicted by the rule of mixtures. These results could be accounted for by one or more of the following factors:

1. Some fraction of the compound layers are cracked and therefore do not make the expected contribution to the modulus.
2. The composition of the compound layers deviates from that expected on the basis of the target construction, and the actual composition results in a smaller amount of the high modulus compound.
3. The compound layer does not exhibit the expected high modulus.

The present deposits do not permit the necessary data to evaluate the importance of these factors. Some of the deposits to be made in the next phase of this program will contain thick enough compound layers to provide such data.

The fracture surfaces of the tensile specimens were examined by scanning electron microscopy (SEM) to determine whether the brittle behavior was the result of growth defects not visible at the deposit surface. A typical set of photographs is shown in Figure 13 for deposit 24/0.2. This deposit had one unintentional deposit-deposit interface resulting from a momentary interruption of the deposition process, Figure 13a. Several defects are visible on the fracture surface of the larger portion of the deposit which began at this interface. The fracture appears to have been initiated at the defect near the center of the specimen width. This is tentative, however, since the fracture markings are not as clearly directional as those in conventional materials.

The higher magnification photographs, Figures 13b and c suggest that the fracture path follows the boundaries of the columnar growth structure of the deposit. This structure is not to be confused with the grain structure, which is one to two orders of magnitude smaller. The columnar growth structure is typical of unannealed sputtered deposits, and other vapor deposits as well. Its boundaries consist of material deposited under partially shadowed geometry, which results in less than theoretical density and reduced strength.

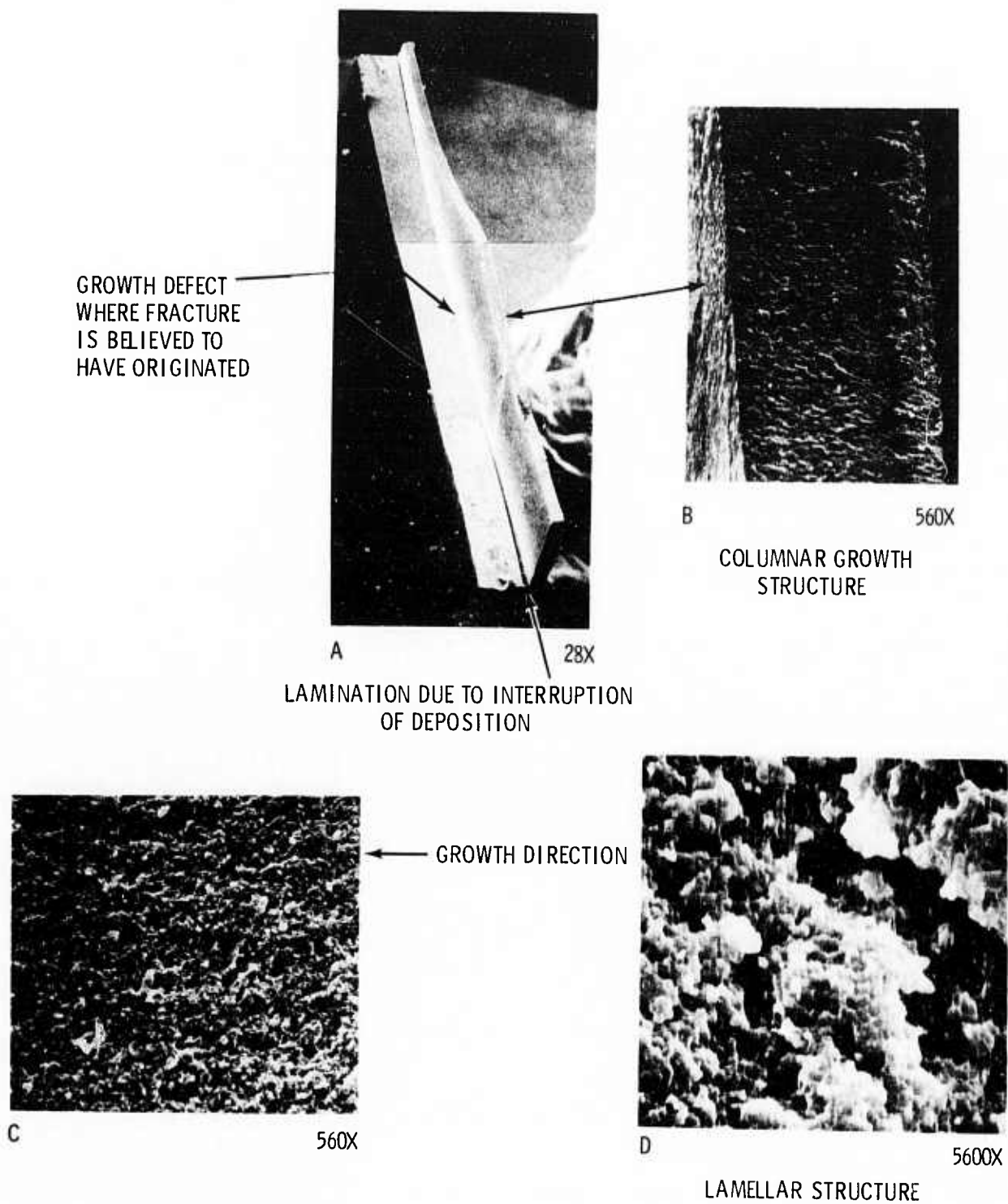


FIGURE 13. Fracture Surface of Tensile Specimen from Deposit 24/0.2. Scanning Electron Micrographs. Note Absence of Delamination in D.

The lamellar structure is visible in the highest magnification photograph, Figure 13d. No separation of the layers is visible, indicating that a high degree of interfacial strength has been obtained.

Three samples were tested in tension at 450°C in flowing argon, in an effort to obtain sufficient plasticity to derive meaningful tensile strengths. Two of these samples exhibited plastic strains estimated (from cross head travel) at >0.2%, and ultimate tensile strengths of 497 and 532 kg/cm² (71 and 76 ksi). It was not possible to obtain useful offset yield strengths since strain gauges were not used.

Three Point Bending

The results of tests in three point bending are presented in Table X.

TABLE X. Bend Test Results

Deposit	Heat Treatment*	Maximum Fiber Stress at Strain of:					
		1×10^{-4}		4×10^{-4}		2×10^{-3}	
		10^3 kg/cm ²	10^3 psi	10^3 kg/cm ²	10^3 psi	10^3 kg/cm ²	10^3 psi
24/0.2	AD**	12.51	177.5	-	-	-	-
	700	9.04	128.3	-	-	-	-
	800	9.69	137.6	-	-	-	-
14/0.2	AD**	16.15	229.2	18.8	267	-	-
	700	18.35	260.4	21.2	301	26.4	374
	800	8.45	120.0	10.9	155	14.4	205
14/0.1	AD**	16.24	230.5	19.0	270	-	-
	700	20.23	287.1	24.6	349	28.6	406
	800	18.57	263.4	20.2	286	23.2	329
	900	6.20	88.0	7.5	107	9.7	137
24/0.1	AD**	18.92	268.5	22.1	314	-	-
	700	16.11	228.7	-	-	-	-
	800	16.79	238.3	-	-	-	-

* One hour at temperature

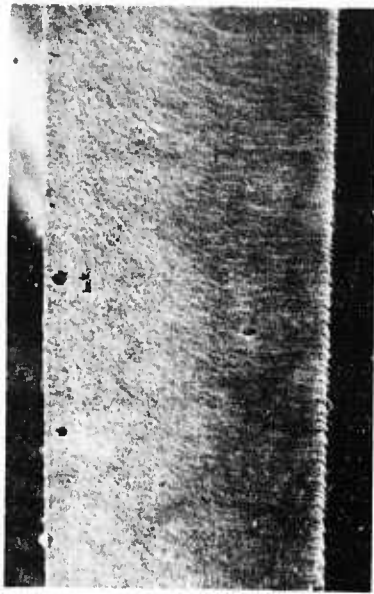
** As deposited

The maximum fiber stress at various strains was obtained by assuming a linear relationship between strain and sample deflection. While not strictly valid, this assumption should not produce large errors for strains of 0.2% or less.

The most significant observation to be made from the data is that samples 14/0.2 and 14/0.1, which have compound layers of 14% relative thickness, developed considerably more plastic strain than the 24% relative thickness samples. Also, the smaller repeating layer thickness samples, 14/0.1 and 24/0.1, developed higher strengths at equal strains. These variations are in the expected directions, and serve to indicate that the lamellar structure of these deposits is in fact controlling the mechanical properties.

The fracture surfaces of as-deposited bend specimens of deposits 14/0.1 and 24/0.1 are illustrated in Figure 14. These deposits differ only in the thickness of the intermetallic compound layer, and fractured at similar strains ($\sim 4 \times 10^{-4}$). The strength of the 24% relative compound layer thickness deposit (Figure 14b) was about 16%, or 308 kg/cm^2 (44 ksi) greater. The fracture surface of this deposit has a larger shear lip and fewer visible defects. Also, the surface topography is considerably smaller in areal dimension. The lamellar structure was not resolved in these specimens, although it was an order of magnitude larger than the claimed resolution of the microscope.

The effect of heat treatment was, in general, small for temperatures below 900°C (one hour treatments). The one sample tested after a 900°C treatment showed a large reduction in strength, which is believed



80X



a) 14/0.1
Growth Direction
→

4000X

Shear Lip
↓



80X



b) 24/0.1
Growth Direction
→

4000X

FIGURE 14. Fracture Surfaces of Bend Specimens from Deposits:
a) 14/0.1, b) 24/0.1. Scanning Electron Micrographs

to be related to the breakup of the lamellar structure by diffusional processes. Support for this was obtained from metallography of another sample heat treated at 950°C, Figure 15, where the breakup is well advanced. This effect was not expected on the basis of the equilibrium diagram. (15)

Microhardness measurements were made as a function of heat treatment for all deposits. The data is illustrated in Figure 16. The 24% relative thickness deposits are significantly harder for all heat treatments, as expected. No consistent effect of the repeating unit layer thickness was observed. The hardness decreased most rapidly during the 900°C treatment, probably due to the breakdown of the lamellar structure. Except for the absence of an effect due to the repeating unit layer thickness, the hardness results were similar to the bend test results.

General Evaluation

Chemical analysis by the atomic absorption method yielded an average result of 7.85 ± 0.06 weight % beryllium for deposit 24/0.2. The nominal composition of this deposit, according to the observed layer thickness and the assumed TiBe_{12} compound, was 9.9 wt% beryllium. These results suggest that the most likely compound is $\text{Ti}_2\text{Be}_{17}$. If this is confirmed by x-ray diffraction (of deposits with thicker compound layers) the configuration of the sputtering target will be appropriately modified.

A sample of deposit 24/0.2 was heated at 40°C/min in a differential scanning calorimeter to look for a potential heat effect due to formation of the intermetallic compound. A small heat effect was observed, beginning at 650°C and completed by 700°C, however this amounted to only

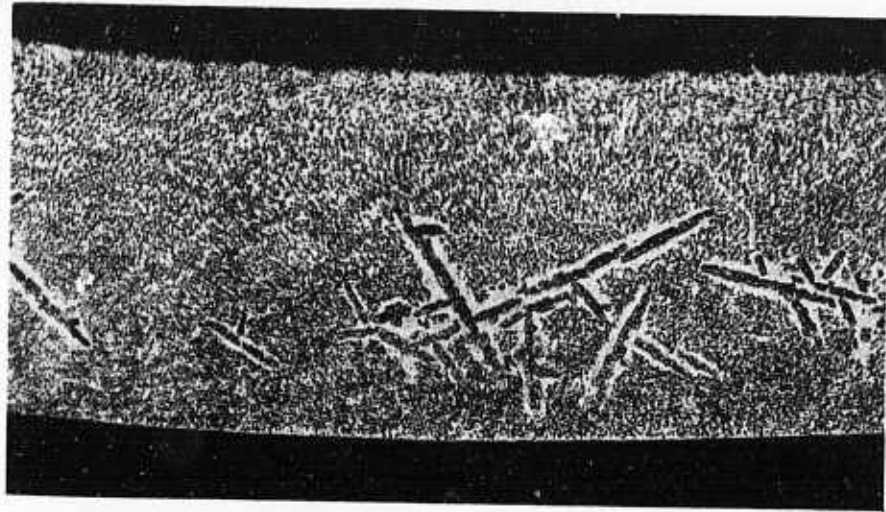


FIGURE 15. Cross Section of Deposit After Heat Treatment at 950°C for One Hour. The Lamellar Structure Has Broken Up By Diffusional Processes. Optical Micrograph 100X.

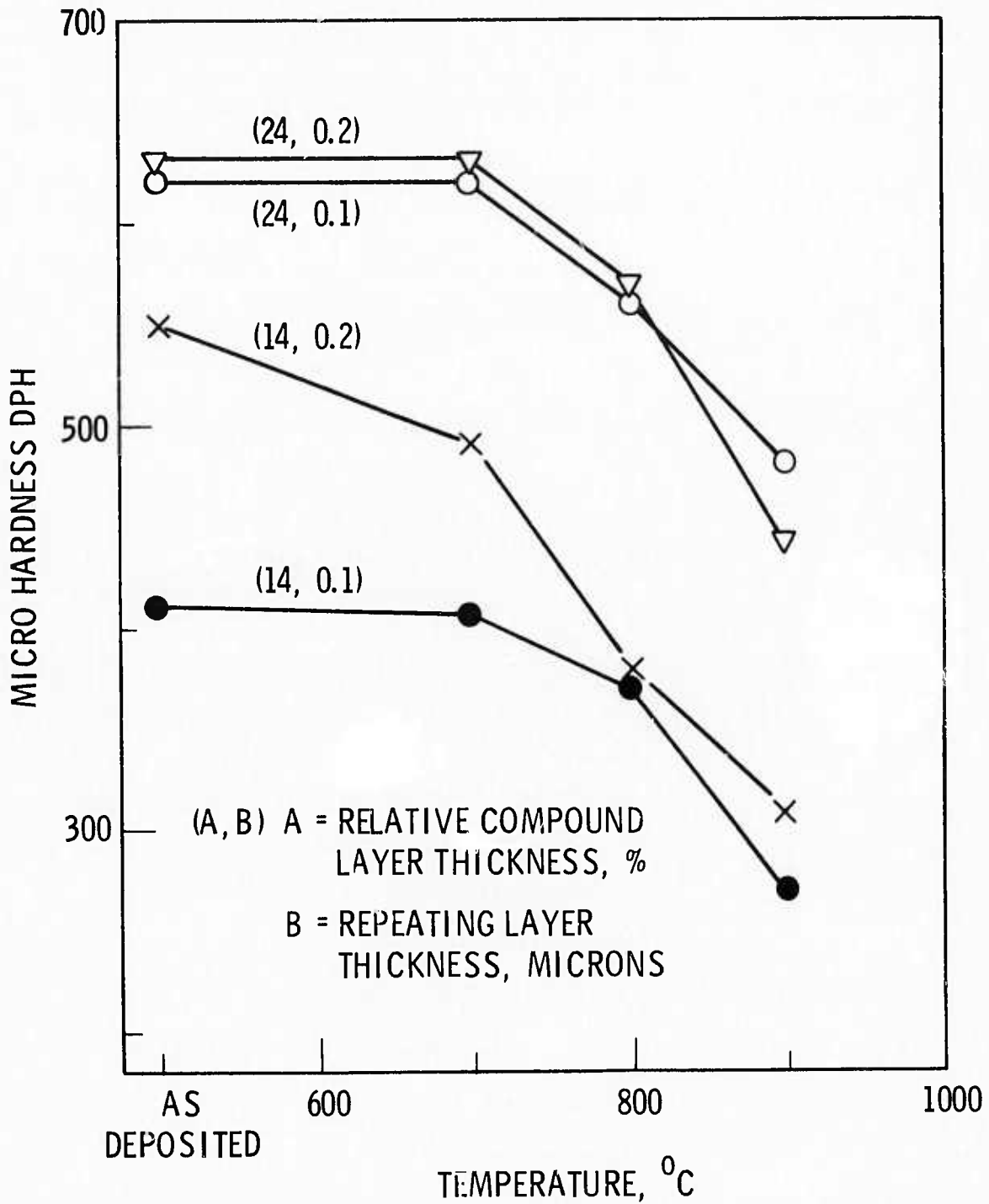


FIGURE 16. Microhardness of Lamellar Composites as a Function of Heat Treatment.

24 calories/mole of compound. It was concluded that the compound had been formed during deposition, and the observed heat effect was a strain relaxation. The alternative conclusion (that the compound did not form either during deposition or in the calorimeter) is unlikely since no significant change in tensile properties was observed with heat treatment up to the point where the lamellar structure broke up.

Sample 14/0.1 was selected for study by electrical resistivity on the basis of its superior performance in mechanical property testing. The results of measurements made at 295 and 77°K before and after one hour heat treatments at the indicated temperatures are presented in Table XI.

TABLE XI. Electrical Resistivity of Deposit 14/0.1 as a Function of Heat Treatment

<u>Condition</u>	<u>Resistivity, Microhm-cm</u>		<u>Ratio*</u>
	<u>295°K</u>	<u>77°K</u>	
As Deposited (500°C)	50.22	13.82	0.275
700°C	56.93	14.85	0.261
800°C	61.93	17.10	0.276
900°C	70.15	21.08	0.300
1000°C	102.88	49.98	0.486

* Ratio = resistivity at 77°K/resistivity at 295°K

These results confirmed that the lamellar composite was stable to 800°C, began to break down at 900°C, and changed rapidly at 1000°C. This behavior is consistent with the hypothesis that the intermetallic compound was formed during deposition rather than during postdeposition heat treatment.

The attempts to observe the kinetics of the resistivity change during heat treatments at 700-900°C were unsuccessful. The resistivity at the heat treatment temperature was essentially constant with time after an initial transient which was ascribed to the temperature equilibration of the sample. The structure was in fact changing as indicated by the changes in the room temperature resistivity after these treatments, (see Table XI). The contribution of these changes to the specimen resistivity, however, was too small a fraction of the (large) total resistivity at temperature to be observed.

Assuming that the resistivity values at the various temperatures refer to the same (as-deposited) structure, for the reasons given above, the resistivity versus temperature characteristic of the material can be obtained. The average temperature coefficient of resistivity (above room temperature) was $3.6 \times 10^{-3} \text{ } ^\circ\text{C}^{-1}$ which is typical of pure metals, and indicates that the pure titanium layers are controlling the resistivity behavior.

REFERENCES

1. J. S. Koehler, "Attempt to Design a Strong Solid," Phys. Rev., B2, 547 (1970).
2. W. A. Jesser and J. W. Mathews, "Evidence for Pseudomorphic Growth of Iron on Copper," Phil. Mag., 15, 1097 (1967).
3. W. A. Jesser and J. W. Mathews, "Pseudomorphic Deposits of Chromium on Nickel," Phil. Mag., 17, 475 (1968).
4. J. W. Mathews and W. A. Jesser, "Study of the F.C.C. to B.C.C Transformation in Films of Iron or Nickel," Phil. Mag., 20, 999 (1969).
5. J. W. Patten, E. D. McClanahan, and J. W. Johnston, "Room Temperature Recrystallization in Thick Bias - Sputtered Copper Deposits," J. Appl. Phys., 42, 4371 (1971).
6. R. A. Busch and J. W. Patten, "Lamellar Composites Formed by Sputter Deposition," Semiannual Technical Report: December 1973, Sponsored by Advanced Research Projects Agency, Contract No. F44620-73-C-0071, ARPA Order No. 2482, Program Code No. 3D10, Battelle Northwest Laboratories, Richland, Washington.
7. Hot Hardness Measurements by Prof. J. Moteff, University of Cincinnati.
8. George E. Dieter, Jr., Mechanical Metallurgy, McGraw-Hill Book Co., Inc., New York, 1961, p. 288.
9. Metals Handbook, Vol. 1, 8th Edition, American Society for Metals, Metals Park, Ohio, 1961, p. 1008.
10. W. Sheithauer, Jr., R. F. Cheny, and N. E. Kopatz, The Manufacture, Properties, and Applications of High-Conductivity High-Strength Cu-ThO₂, CDA-ASM Conference on Copper, Oct. 16-19, 1972, Cleveland, Ohio. Reprinted by Cu Development Corp.
11. Ordinance Metals Handbook, Copper and its Alloys, ORD p. 20-302, Department of the Army, Ordnance Corps, August 1956.
12. W. D. Klopp and W. R. Witzke, Met. Trans., 1973, Vol. 4, p. 2007.

13. From Arc Cast Molybdenum and its Alloys, Climax Molybdenum Company, New York, 1955.
14. W. J. McGregor Tegart, Elements of Mechanical Metallurgy, The MacMillan Co., New York, 1966, p. 89.
15. R. P. Elliot, "Constitution of Binary Alloys," First Supplement, McGraw-Hill Book Co., Inc., New York, 1965, p. 173.